Matched-Line Directional Dividers

Thomas J. Russell, *Member, IEEE*

Abstract— **A new class of passive microwave devices is described that provides for equal or unequal division of a signal from an input to two or more outputs—with the outputs isolated from each other. The matched-line directional divider consists of an input network connected through interconnection ports to a transmission line network. The input network typically consists of resistors. The transmission line network consists of generally parallel transmission lines that are coupled together at the interconnection ports and uncoupled at their output ports. Output match and isolation between output ports is obtained by designing the transmission line network to match the uncoupled output ports to the outputs of the input network. It is shown that by using tapered transmission lines, MLDD's can be designed to have high-pass frequency response. Five new types of coupled tapered line power dividers having terminating resistor configurations at the coupled line inputs are described.**

I. Introduction

MICROWAVE directional devices are useful in a wide variety of instrumentation and system applications. The passive linear devices discussed here have one input and two or more outputs, with the outputs isolated from each other. These include the familiar Wilkinson–Cohn power dividers and TEM mode contradirectional couplers [1]–[3]. This paper introduces a new class of these devices that use coupled transmission lines—which we will designate matched-line directional dividers. It is assumed that the transmission lines are lossless, and coupling is TEM mode or quasi-TEM mode as defined by Krage *et al.* [4].

II. General Analysis

A general schematic of the MLDD is shown in Fig. 1. The device consists of an input network and transmission line network. The input network includes N signal paths from its input to N interconnection ports $(ii_1, ii_2, \cdots, ii_n)$ that are connected to N interconnection ports $(ti_1, ti_2, \cdots, ti_n)$ of the transmission line network. The input network is typically, but not always, a resistor network and includes at least $N-1$ resistors, each of which has at least one end connected to a different interconnection port. The transmission line network consists of N generally parallel transmission lines that are coupled together at the transmission line network inputs and connected at their opposite ends to output ports $(to_1, to_2, \cdots, to_n)$.

At any location x, the electrical characteristics of the transmission lines can be expressed in terms of the elements of their inductance $[L(x)]$ and capacitance $[C(x)]$ matrices. For a homogeneous dielectric only $[C(x)]$ and the propagation velocity v are needed since, then,

$$[L(x)] = \frac{[C(x)]^{-1}}{v^2}. \tag{1}$$

Matched and isolated output ports are obtained by:

1) designing the transmission line network to transform from the uncoupled output port impedances to the coupled line cross section at $x = 0$; and

2) designing the input network so that its output conductance matrix $[G]$ provides a reflectionless termination for all signals incident from the input of the transmission line network.

Amemiya [5] has elegantly proved the general realizability of $[G]$ with a resistive network, which he calls a matched termination network. Except for not being unique, the matched termination network is analogous to the characteristic impedance of a single transmission line. In [5] it is shown that

$$[G] = [C(0)][V]_m[v(0)][V]_m^{-1} \tag{2}$$

where

$$[v(0)] = \begin{bmatrix} v(0)_1 & 0 & 0\cdots 0 \\ 0 & v(0)_2 & 0\cdots 0 \\ 0 & 0 & v(0)_3\cdots 0 \\ \vdots & & \\ 0 & 0 & 0\cdots v(0)_n \end{bmatrix} \tag{3}$$

with

$$v(0)_i = \text{velocity of propagation of the } i\text{th mode}$$

and

$$v(0)_i = \frac{1}{\sqrt{\sigma_i}} \text{ where the } \sigma_i \text{ are eigenvalues of } [L(0)][C(0)]$$

and

$$[V]_m \text{ is a modal matrix made of } n \text{ different eigenvectors of } [L(0)][C(0)].$$

For TEM mode propagation, (2) reduces to

$$G = v[C(0)] \tag{4}$$

where v is the velocity of propagation in the medium.

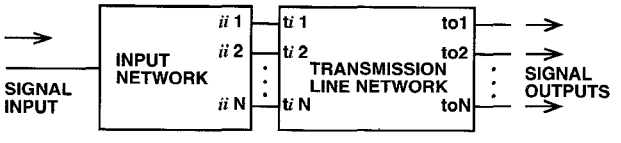

Fig. 1. General schematic of matched-line directional divider.

Manuscript received July 2, 1992; revised November 5, 1992.
The author is with KRYTAR, Sunnyvale, CA 94089.
IEEE Log Number 9209336.

Assuming a resistive input network, the bandwidth of the MLDD is equal to the bandwidth of the transmission line network. The impedance transformation of the transmission line network can be realized by stepped or tapered transmission line structures. A tapered line structure has the advantage of giving a high-pass response.

Fig. 2 illustrates circuit topologies and corresponding suitable transmission line network structures for five types of MLDD's.

III. Type 1 MLDD

This type of MLDD is a 2-way equal division in-phase power divider. Due to symmetry, this device can be conveniently analyzed with the even-mode and odd-mode equivalent circuits of Fig. 3. A tapered line network transforms the even mode impedance from 50 Ω at $x = l$ to $100 + R$ Ω at $x = 0$. The odd-mode impedance is transformed from 50 Ω at $x = l$ to R Ω at $x = 0$. The output reflection coefficient (ρ_{out}) and isolation are given by

$$\rho_{out} = (\rho_e + \rho_o)/2 \tag{5}$$

$$\text{isolation} = 20 \log\left\{\frac{2}{|\rho_e - \rho_o|}\right\} \tag{6}$$

where ρ_e and ρ_o are the output even-mode and odd-mode reflection coefficients. The even-mode impedance $Z_e(x)$ and odd-mode impedance $Z_o(x)$ at a location x are given by

$$Z_e(x) = \frac{1}{vC_1(x)} \tag{7}$$

$$Z_o(x) = \frac{1}{v(C_1(x) + 2C_{12}(x))} \tag{8}$$

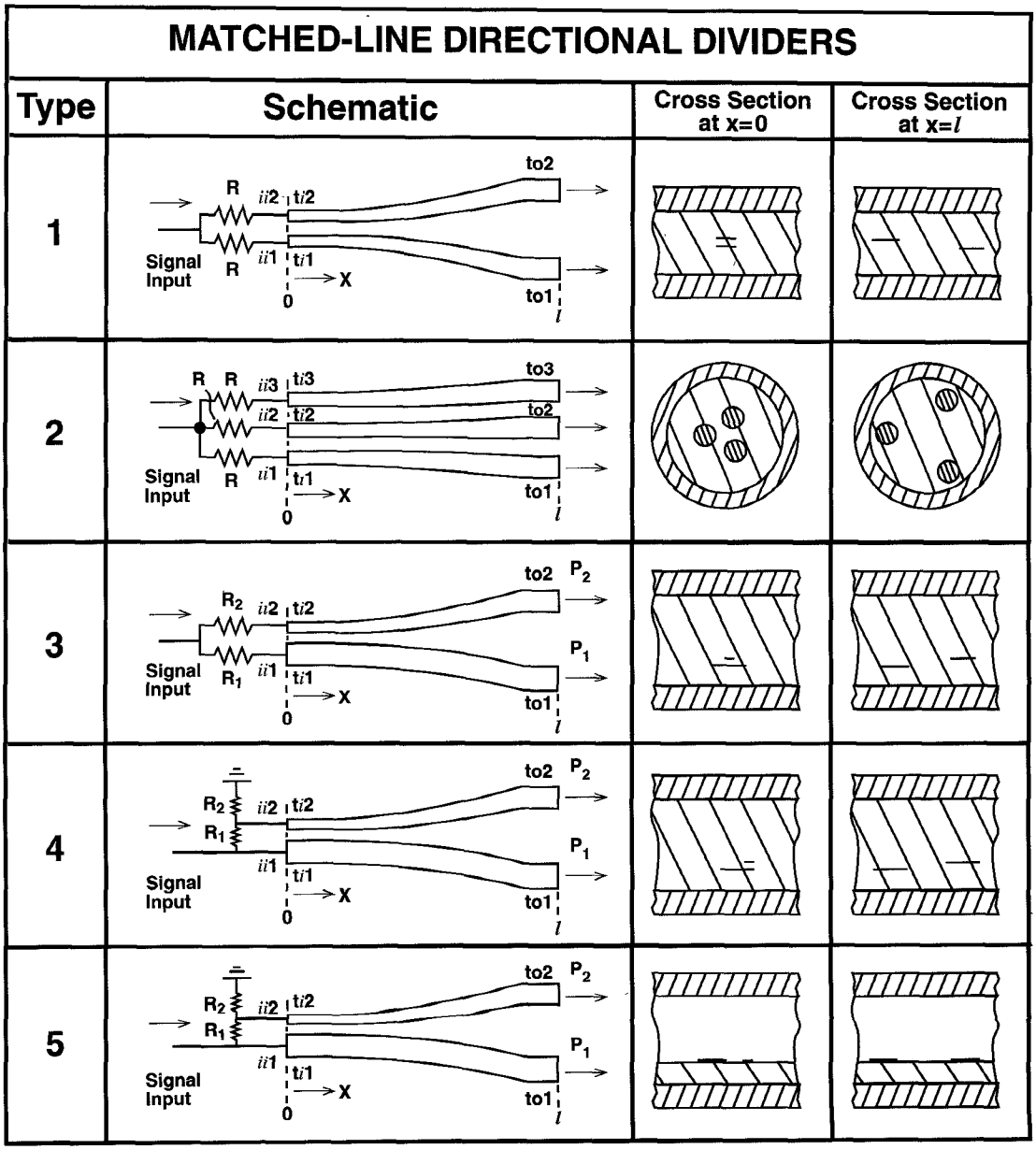

Fig. 2. Five types of matched-line directional dividers.

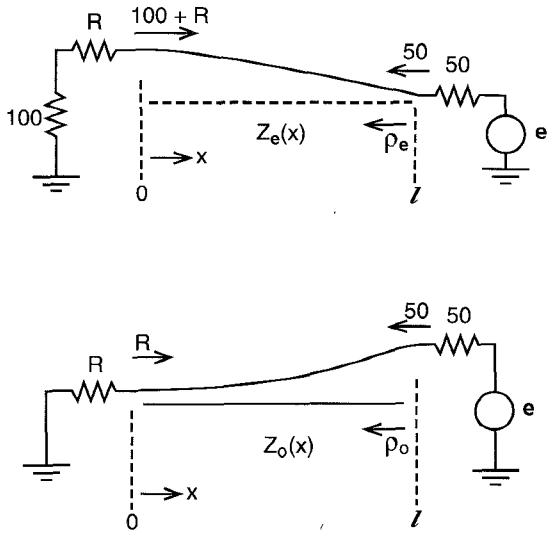

Fig. 3. Type 1 MLDD even-mode and odd-mode equivalent circuits.

where $C_1(x)$ and $C_{12}(x)$ are as shown in Fig. 4, and v is the velocity of propagation in the medium.

In the pass band of the transmission line network, it can be shown that the insertion loss due to power loss in the two resistors is closely approximated by

$$\text{insertion loss} = 10\log(1 + R/100)\,. \tag{9}$$

A useful impedance taper for making the even-mode and odd-mode impedance transformation has been described by Collin [6]. The Collin taper has a high-pass response that gives a reflection coefficient that decreases from a maximum magnitude of ρ_m toward 0 as frequency increases, the rate of decrease depending upon an integer $\overline{n}$. In a practical design, this is more desirable than an equal ripple design [7], since the decreasing reflection coefficient compensates for the typically increasing reflections with increasing frequency from other parts of the circuit—such as input and output connectors. Using Collin tapers, ρ_{in}, ρ_e, and ρ_o are given by

$$\rho_{in} = \frac{R - 100\rho_e}{R + 100} \tag{10}$$

$$\rho_e = \rho_c\left\{\left(\frac{R+100}{50}\right), \overline{n}, \mu_o, \mu\right\} \tag{11}$$

$$\rho_o = -\rho_c\left\{\left(\frac{50}{R}\right), \overline{n}, \mu_o, \mu\right\} \tag{12}$$

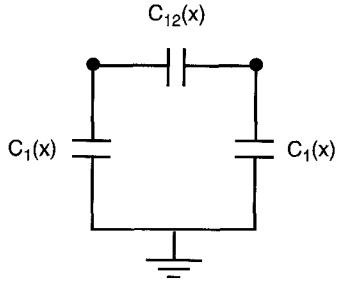

Fig. 4. Coupled-line capacitances.

where

$$\rho_c\{y, \overline{n}, \mu_o, \mu\} = \frac{e^{-j\pi\mu}\ln(y)\sin(\pi\mu)}{2\pi\mu} \cdot \left[\frac{\prod_{n=1}^{\overline{n}-1}\left\{1 - \left(\frac{\mu}{n}\right)^2\left[\frac{\mu_o^2 + \left(\overline{n} - \frac{1}{2}\right)^2}{\mu_o^2 + \left(n - \frac{1}{2}\right)^2}\right]\right\}}{\prod_{n=1}^{\overline{n}-1}\left\{1 - \left(\frac{\mu}{n}\right)^2\right\}}\right] \tag{13}$$

$$\mu_o = \frac{1}{\pi}\cosh^{-1}\left(\frac{\ln(y)}{2\rho_m}\right) \tag{14}$$

$$\mu = \frac{l\sqrt{\epsilon_r}f}{1.5 \times 10^8} \tag{15}$$

l is length in meters and f is frequency in hertz.

Due to symmetry, the two output signals will be theoretically equal in amplitude and phase.

As frequency increases in the pass band, ρ_e approaches 0, and from (10) it is seen that ρ_{in} approaches $R/(R + 100)$, which corresponds to an input VSWR of $1 + R/50$.

Fig. 5 shows theoretical input VSWR, output VSWR, and isolation from 0.5–10 GHz for the type 1 MLDD with

$$l = 188 \text{ mm}$$
$$\epsilon_r = 2.1$$
$$R = 10\ \Omega$$
$$\rho_m = 0.075$$
$$\overline{n} = 10\,.$$

Substituting $R = 10$ in (9) gives a pass band insertion loss of 0.41 dB.

This example was fabricated using 1.016-mm-thick teflon outer dielectric boards and centerboard of 0.127-mm-thick Rogers 5880 Duroid. The coupled lines were etched from 1/2-oz rolled copper laminated to opposite sides of the centerboard. At the input of the transmission line network, the conductors have widths of 1.321 mm, and one conductor is directly over the other one—to give an even-mode impedance of 110 Ω and odd-mode impedance of 10 Ω. At the output of the transmission line network, the two lines are a maximum distance apart and have widths of 1.829 mm to give 50 Ω characteristic impedance. The width of the input line is 1.575 mm to give 50 Ω characteristic impedance. The two resistors were "chip" resistors made of 0.254-mm-thick aluminum nitride with a tantalum nitride resistive film. As shown in Fig. 6, the two resistors are soldered across 0.381 mm gaps in the strip transmission lines and connected together on the input end by two 0.457-mm-diameter plated through holes. Measured values of input VSWR, output VSWR, insertion loss, isolation, amplitude tracking, and phase tracking are shown in Fig. 7. The increasing insertion loss (above the theoretical 0.41 dB) with increasing frequency is due to dielectric and copper losses not considered in the analysis.

IV. Induced Coupling in Parallel Transmission Lines

One of the more intriguing characteristics of the type 1 MLDD is that it operates contrary to generally accepted theory.

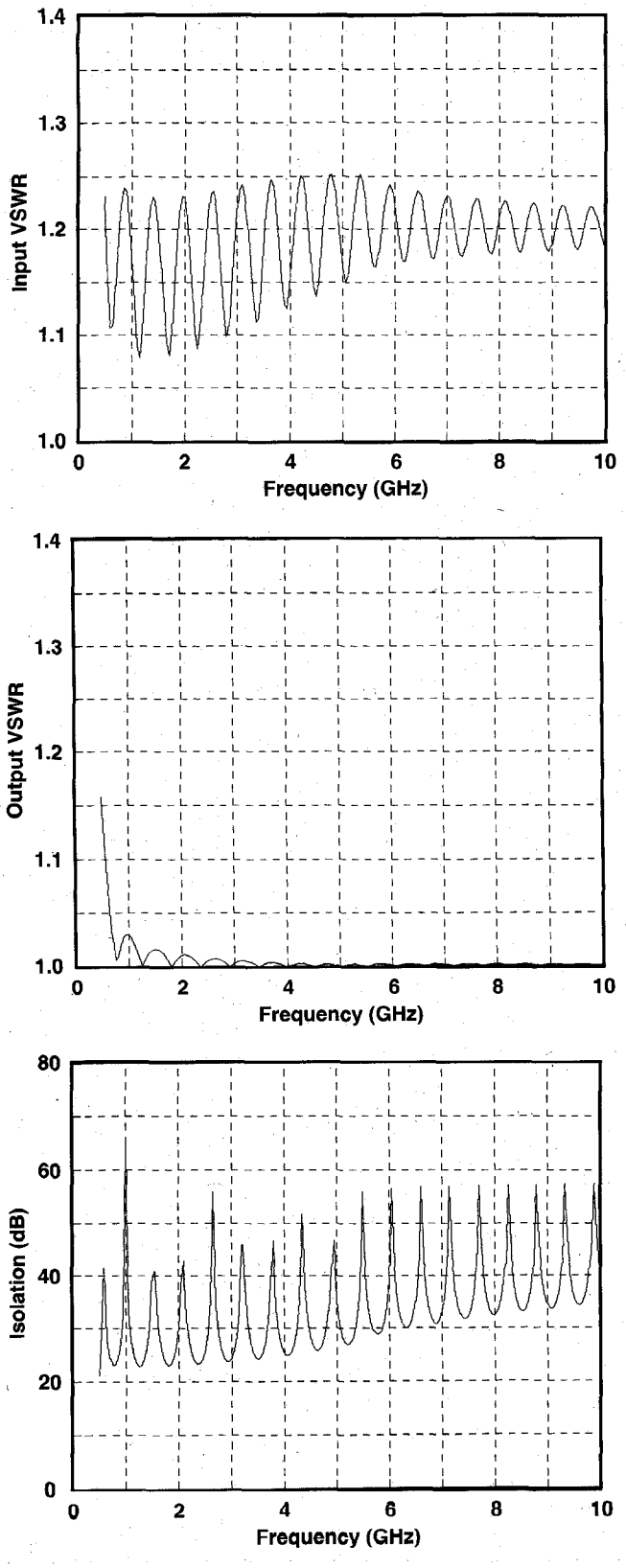

Fig. 5. Theoretical input VSWR (top), output VSWR (middle), and isolation (bottom).

It appears to be generally believed [3], [4], [8] that coupling between TEM or quasi-TEM mode coupled lines is inherently contradirectional. That is, a signal propagating on one of the lines will induce a signal propagating in the opposite direction

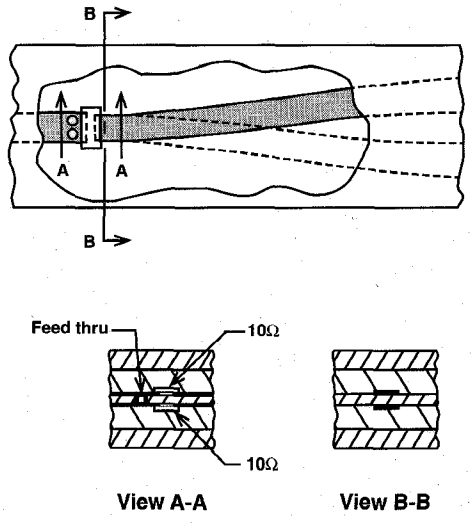

Fig. 6. Two-way stripline type 1 MLDD configuration.

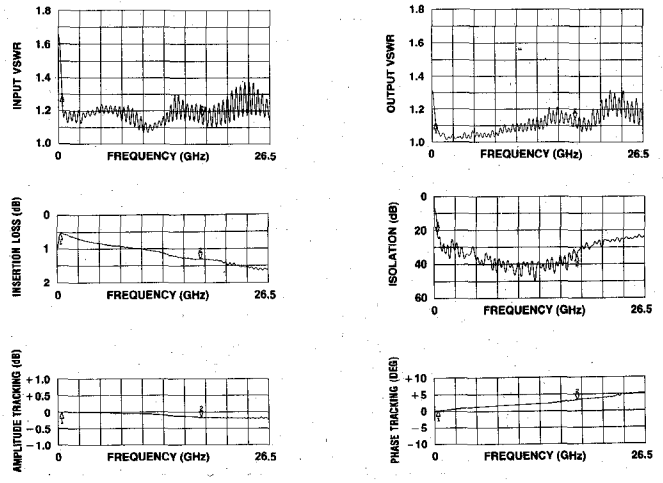

Fig. 7. Measured performance of type 1 MLDD. Markers are at 0.5 and 18 GHz.

on the other line. Yet, although the coupled lines of the type 1 MLDD are generally parallel, a signal in one output port does not induce a signal exiting the other output port.

Fig. 8 shows a pair of lossless TEM or quasi-TEM mode parallel coupled transmission lines terminated in a network Z. We will specify Z to be the matched termination network described by Amemiya. This is analogous to terminating a single transmission line by its characteristic impedance, and equivalent to extending the parallel lines to infinity. There will then be no reflected waves, and hence no induced contradirectional signal. Voltages and currents of the remaining forward waves on the two lines can be expressed by [9], [10]

$$v_1 = A_1 e^{-j\beta_c x} + A_3 e^{-j\beta_\pi x} \tag{16}$$

$$v_2 = A_1 R_c e^{-j\beta_c x} + A_3 R_\pi e^{-j\beta_\pi x} \tag{17}$$

$$I_1 = A_1 Y_{c1} e^{-j\beta_c x} + A_3 Y_{\pi 1} e^{-j\beta_\pi x} \tag{18}$$

$$I_2 = -\frac{A_1 Y_{c1}}{R_\pi} e^{-j\beta_c x} - \frac{A_3 Y_{\pi 1}}{R_c} e^{-j\beta_\pi x} \tag{19}$$

where β_c, β_π, R_c, R_π, Y_{c1} and $Y_{\pi 1}$ are normal mode parameters of the coupled lines. For TEM mode transmission $\beta_c = \beta_\pi$ and $R_\pi = -R_c$.

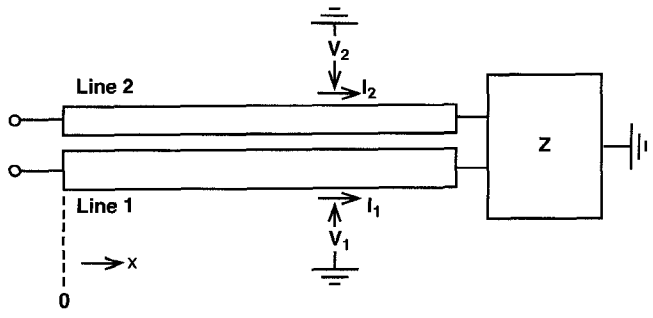

Fig. 8. Two coupled transmission lines terminated with a network Z.

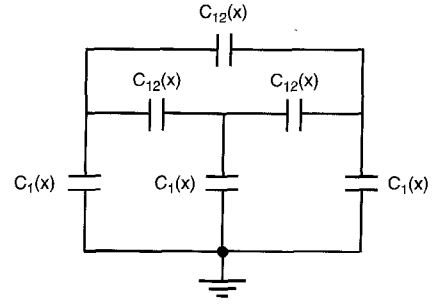

Fig. 9. Coupled-line capacitances.

From (16)–(19), it can be shown that

$$\begin{bmatrix} V_2 \\ I_2 \end{bmatrix} = \begin{bmatrix} \frac{R_c Y_{\pi 1} - R_\pi Y_{c1}}{Y_{\pi 1} - Y_{c1}} & \frac{R_\pi - R_c}{Y_{\pi 1} - Y_{c1}} \\ \frac{\frac{1}{R_c} - \frac{1}{R_\pi}}{\frac{1}{Y_{c1}} - \frac{1}{Y_{\pi 1}}} & \frac{\frac{Y_{c1}}{R_\pi} - \frac{Y_{\pi 1}}{R_c}}{Y_{\pi 1} - Y_{c1}} \end{bmatrix} \begin{bmatrix} V_1 \\ I_1 \end{bmatrix}. \quad (20)$$

A forward wave on line 1 clearly induces a codirectional signal on line 2, with the voltages and currents of line 2 related to those of line 1 by (20). The well-known TEM-mode contradirectional couplers are contradirectional because of reflections in the two-line system.

V. Type 2 MLDD

This type of MLDD is a 3-way equal division in-phase power divider. Due to symmetry, this device can also be analyzed with an even-mode odd-mode analysis. The even-mode analysis is implemented by applying $+1/3$ V through a 50 Ω impedance to each output. The odd-mode analysis applies $+2/3$ V through 50 Ω to one output and $-1/3$ V through 50 Ω to each of the other two output ports. The output reflection coefficient (ρ_{out}) and isolation are given by

$$\rho_{out} = \frac{\rho_e}{3} + \frac{2\rho_o}{3} \quad (21)$$

$$\text{isolation} = 20 \log\left\{\frac{3}{|\rho_e - \rho_o|}\right\} \quad (22)$$

with the even-mode impedance $Z_e(x)$ and odd-mode impedance $Z_o(x)$ at a location x given by

$$z_e(x) = \frac{1}{vC_1(x)} \quad (23)$$

$$z_o(x) = \frac{1}{v(C_1(x) + 3C_{12}(x))} \quad (24)$$

where $C_1(x)$ and $C_{12}(x)$ are as shown in Fig. 9 and v is the velocity of propagation in the medium. The transmission line network transforms the even-mode impedance from 50 Ω to $Z_e(0) = 150 + R$ and the odd-mode impedance from 50 Ω to $Z_o(0) = R$.

In the pass band of the transmission line network, it can be shown that the insertion loss due to power loss in the two resistors is closely approximated by

$$\text{insertion loss} = 10 \log(1 + R/150). \quad (25)$$

Again, using Collin impedance tapers, ρ_{in}, ρ_e, and ρ_o are given by

$$\rho_{in} = \frac{R - 150\rho_e}{R + 150} \quad (26)$$

$$\rho_e = \rho_c\left\{\left(\frac{R+150}{50}\right), \overline{n}, \mu_o, \mu\right\} \quad (27)$$

$$\rho_o = -\rho_c\left\{\left(\frac{50}{R}\right), \overline{n}, \mu_o, \mu\right\} \quad (28)$$

with ρ_c, μ_o, and μ as given by (13), (14), and (15).

Due to symmetry, the output signals will again be theoretically equal in amplitude and phase.

As frequency increases in the pass band, ρ_e approaches 0 and, from (26), it is seen that ρ_{in} approaches $R/(R+150)$, which corresponds to an input VSWR of $1 + R/75$.

Equations (21), (22), and (26) give high-pass performance similar to that of Fig. 5.

VI. Type 3 MLDD

This type of MLDD gives unequal power division and in-phase outputs. The network of Fig. 10 is seen looking toward the output of the input network. The cross section transmission line capacitances at a location x are shown in Fig. 11(a). Since the medium is homogeneous, these capacitances are related to the conductance matrix $[G(x)]$ by (4). $[G(x)]$ can be realized by a resistive T or π network. We choose to use the π network

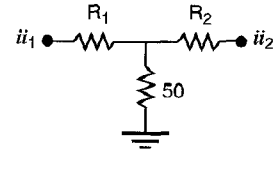

Fig. 10. Network looking toward output of input network.

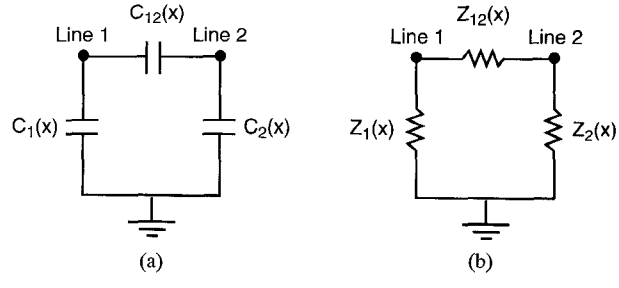

Fig. 11. (a) Coupled-line capacitances and (b) characteristic $\pi(x)$ network.

and will refer to it as $\pi(x)$, the characteristic π network. $\pi(x)$ at a location x is shown in Fig. 11(b) with

$$C_1(x) = \frac{1}{vZ_1(x)} \tag{29}$$

$$C_{12}(x) = \frac{1}{vZ_{12}(x)} \tag{30}$$

$$C_2(x) = \frac{1}{vZ_2(x)}. \tag{31}$$

It can also be shown that the normal mode parameters are given by $\beta(x) = \beta_c(x) = \beta_\pi(x)$, $R(x) = R_c(x) = -R_\pi(x)$, and

$$R(x) = \sqrt{\frac{Z_2(x)(Z_1(x) + Z_{12}(x))}{Z_1(x)(Z_2(x) + Z_{12}(x))}} \tag{32}$$

$$Z_{c1}(x) = \frac{Z_1(x)Z_{12}(x)}{Z_{12}(x) - (R-1)Z_1(x)} \tag{33}$$

$$Z_{\pi 1}(x) = \frac{Z_1(x)Z_{12}(x)}{Z_{12}(x) + (R+1)Z_1(x)} \tag{34}$$

$$Z_{c2}(x) = [R(x)]^2 Z_{c1}(x). \tag{35}$$

As x varies from 0 to l, $\pi(x)$ is varied continuously from $\pi(0)$ to $\pi(l)$. $\pi(0)$ is the π network equivalent of the network of Fig. 10.

It is convenient to divide $Z_{12}(x)$ of Fig. 11(b) into two resistors $Z_{121}(x)$ and $Z_{122}(x)$ according to

$$\frac{Z_{121}(x)}{Z_1(x)} = \frac{Z_{122}(x)}{Z_2(x)}. \tag{36}$$

Then

$$Z_{121}(x) = \frac{Z_1(x)Z_{12}(x)}{Z_1(x) + Z_2(x)}. \tag{37}$$

We also define "odd-mode" impedance $Z_{10}(x)$ according to

$$Z_{10}(x) = \frac{Z_1(x)Z_{121}(x)}{Z_1(x) + Z_{121}(x)} = \frac{Z_1(x)Z_{12}(x)}{Z_1(x) + Z_{12}(x) + Z_2(x)}. \tag{38}$$

$Z_{12}(x)$ is then given by

$$Z_{12}(x) = \frac{Z_{10}(x)(Z_1(x) + Z_2(x))}{Z_1(x) - Z_{10}(x)}. \tag{39}$$

As x varies from 0 to l, $Z_1(x)$, $Z_{10}(x)$, and $Z_2(x)$ are varied continuously from $Z_1(0)$, $Z_{10}(0)$, and $Z_2(0)$ to 50 Ω. $C_1(x)$, $C_{12}(x)$, and $C_2(x)$ can be determined by first calculating $Z_{12}(x)$ from (39) and then using (29)–(31).

In the pass band of the transmission line network, the power loss due to the two resistors is closely approximated by

$$\text{insertion loss} = 10 \log\left\{1 + \frac{R_1 R_2}{50(R_1 + R_2)}\right\}. \tag{40}$$

Also, as frequency increases, the pass band input VSWR approaches

$$\text{input VSWR} = 1 + \left\{\frac{R_1 R_2}{25(R_1 + R_2)}\right\}. \tag{41}$$

Due to lack of symmetry, the type 3 MLDD does not lend itself to a closed form of analysis. The analysis was made using a "brute force" approach with a computer. The transmission line network was divided into 500 constant impedance sections, each of length $500/l$. The ABCD matrix

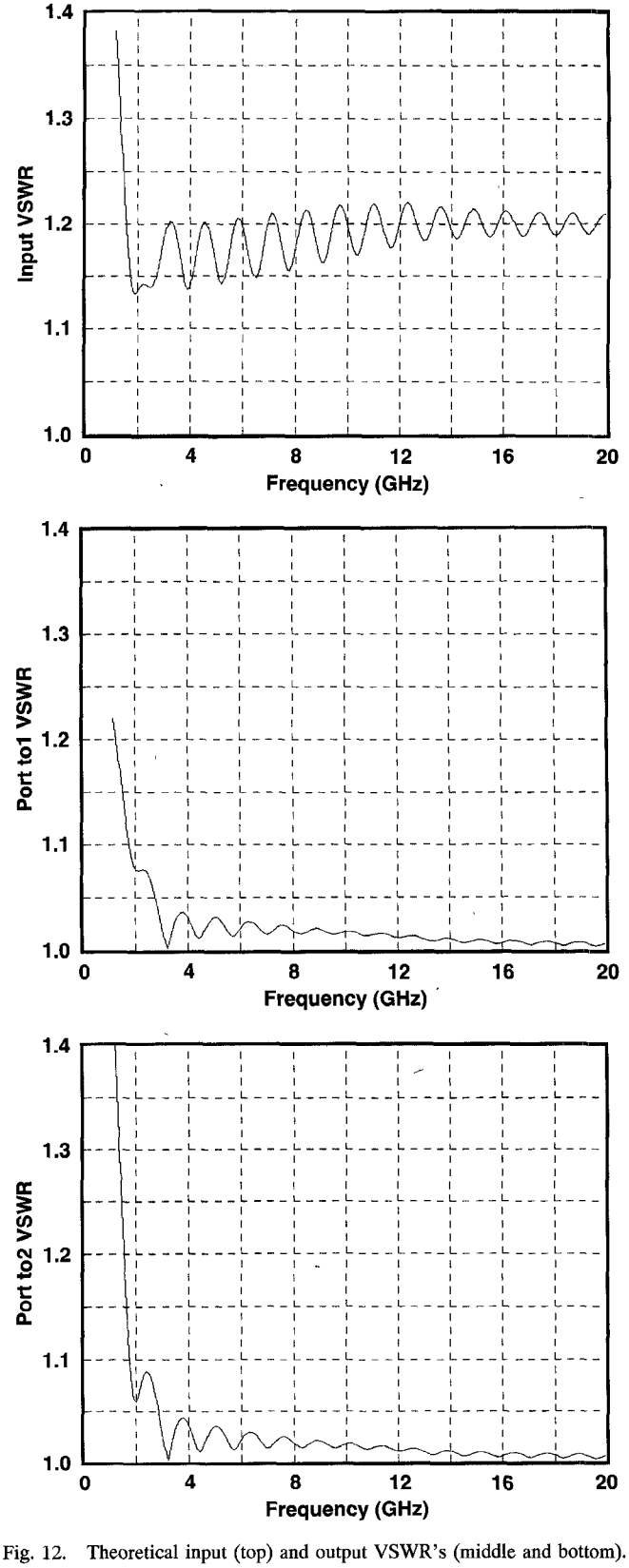

Fig. 12. Theoretical input (top) and output VSWR's (middle and bottom).

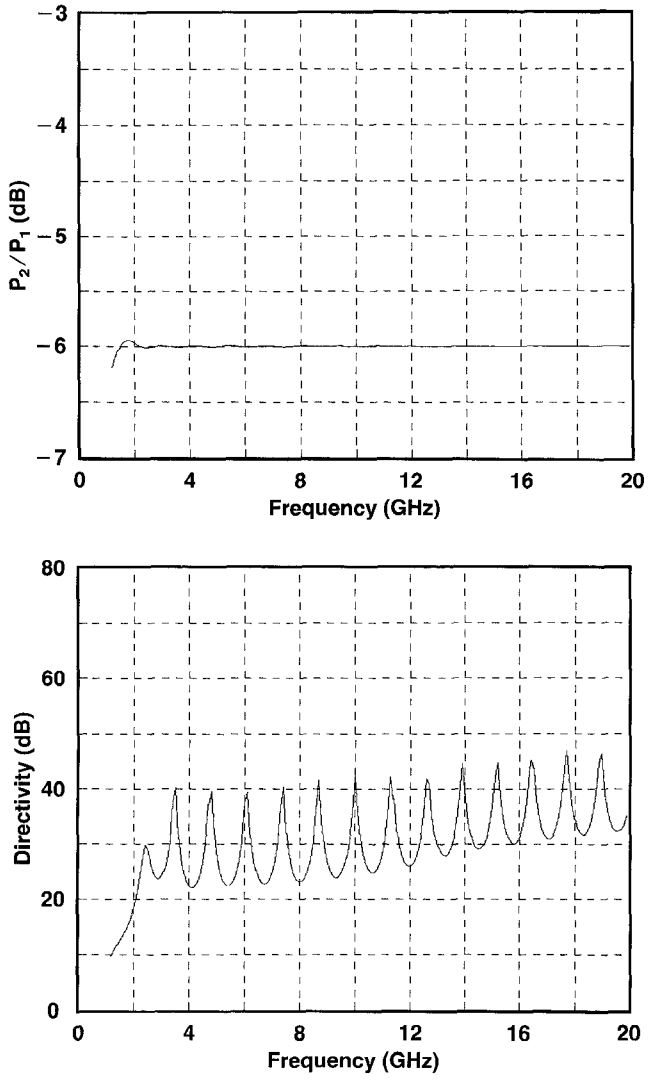

Fig. 13. Theoretical P_2/P_1 (top) and directivity (bottom).

of each section was determined using equations from [10], and the resultant ABCD matrix determined by taking the matrix product of the 500 sections.

Electrical performance was calculated for a design that varied $Z_1(x)$, $Z_{10}(x)$, and $Z_2(x)$ using Collin impedance tapers with $\rho_m = 0.04$, $\overline{n} = 10$, and the following other parameters:

$$l = 80 \text{ mm}$$
$$\epsilon_r = 2.2$$
$$R_1 = 5.36\ \Omega$$
$$R_2 = 75.00\ \Omega.$$

Plots of input VSWR and output VSWR's are shown in Fig. 12. With unequal power division, directivity is generally of more interest than isolation. Plots of P_2/P_1 and directivity are shown in Fig. 13. The response is again high pass with P_2/P_1 constant in the pass band above the low end frequency of 1.4 GHz.

Table I shows values of R_1, R_2, $Z_1(0)$, $Z_{12}(0)$, $Z_2(0)$, and P_2/P_1 for three different designs—including the above example. The parallel combinations of R_1 and R_2 is kept constant at 5 Ω, giving from (40) and (41) pass band insertion loss of 0.41 dB and input VSWR approaching 1.2. Fig. 14(a) shows a cross section corresponding to values of $Z_1(0)$, $Z_{12}(0)$ and $Z_2(0)$, respectively, of 58.93, 88.40, and 824.6 Ω. These line widths were determined by evaluating $C_1(0)$, $C_{12}(0)$, and $C_2(0)$ from (29), (30), and (31), and determining corresponding strip line dimensions using a commercially available software package by Djordjevic *et al.* [13]. The value of pass band coupling is not a unique function of R_1 and R_2—varying with the type of impedance taper used. For example, using linear tapers gives P_2/P_1 values of −2.31, −4.10, and −9.31 dB for the examples of Table I. This type of MLDD is useful for P_2 outputs typically 0 to 6 dB below P_1. For larger ratio's the width of the secondary line tends to become too small to be physically realizable in a practical structure.

VII. Type 4 MLDD

This type of MLDD also gives unequal power division and in-phase outputs.

As x varies from 0 to l, $Z_{10}(x)$ and $Z_2(x)$ are varied continuously from $Z_{10}(0)$ and $Z_2(0)$ to 50 Ω. $Z_1(x)$ is kept constant at 50 Ω. $C_1(x)$, $C_{12}(x)$, and $C_2(x)$ can be calculated in the same manner as for the type 3 MLDD.

In the pass band of the transmission line network, the power loss due to the two resistors is closely approximated by

$$\text{insertion loss} = 10 \log\left\{1 + \frac{50}{R_1 R_2}\right\}. \tag{42}$$

Also, as frequency increases, the pass band input VSWR approaches

$$\text{input VSWR} = 1 + \left\{\frac{100}{R_1 + R_2}\right\}. \tag{43}$$

Electrical performance of the type 4 MLDD is similar to that shown in Fig. 12 and 13 for the type 3 MLDD, except that the ratio of P_2 to P_1 is less.

Table II shows values of R_1 and R_2 for three different designs. The sum of R_1 and R_2 is kept constant at 500 Ω,

TABLE I
VALUES OF R_1, R_2, $Z_1(0)$, $Z_{12}(0)$, $Z_2(0)$, AND P_2/P_1 FOR THREE TYPE 3 MLDD'S

R_1	R_2	$Z_1(0)$	$Z_{12}(0)$	$Z_2(0)$	P_2/P_1	P_2/P_1 (dB)
7.45	15.19	81.97	24.90	167.14	2/3	−1.77
6.46	22.12	71.06	31.44	243.33	1/2	−3.01
5.36	75.00	58.93	88.40	824.63	1/4	−6.02

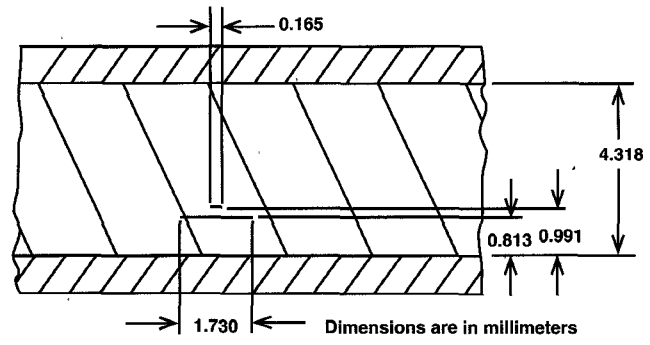

(a)

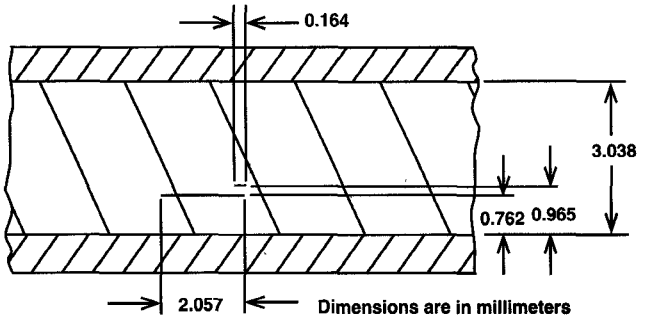

(b)

Fig. 14. Cross sections at $x = 0$ for (a) type 3 and (b) type 4 MLDD's.

TABLE II
VALUES OF R_1, R_2 AND P_2/P_1 FOR THREE TYPE 4 MLDD'S

R_1	R_2	P_2/P_1	P_2/P_1 (dB)
118.0	382.0	1/10	−10.0
209.0	291.0	1/20	−13.0
294.0	206.0	1/40	−16.0

giving from (42) and (43) pass band insertion loss of 0.41 dB and input VSWR approaching 1.2. Fig. 14(b) shows a cross section corresponding to values of $Z_1(0) = 50.00$ ohms, $Z_{12}(0) = R_{12} = 118$ ohms and $Z_2(0) = R_2 = 382$ ohms. This type of MLDD is useful for P_2 outputs 10 dB or more below P_1. For closer coupling values of less than 10 dB the width of the secondary line becomes too small to be physically realizable in a practical structure.

VIII. TYPE 5 MLDD

This type of MLDD gives a typically 55 percent bandwidth 2-way equal division 3 dB 90° hybrid that performs well above 25 GHz and is realizable in microstrip.

This MLDD is the most difficult to analyze theoretically, since the coupled lines are nonsymmetrical and the dielectric is inhomogeneous. An inhomogeneous dielectric is unsuitable for a very broadband divider in this configuration because the different propagation constants β_c and β_π [10, (1)] cause the output power ratio to vary with frequency. In this MLDD, the difference in β_c and β_π is used to obtain much greater power transfer between the coupled lines in the pass band than could be achieved with a conventional edge coupled microstrip contradirectional coupler with similar spacing between the lines.

The pass band insertion loss and VSWR are still closely approximated by (42) and (43).

From (16), (17), (18), and (19), it can be shown that the elements of $[G(x)]$, the conductance matrix corresponding to $\pi(x)$, are given by

$$G_{11}(x) = \frac{R_c(x)Y_{\pi 1}(x) - R_\pi(x)Y_{c1}(x)}{R_c(x) - R_\pi(x)} \tag{44}$$

$$G_{12}(x) = \frac{Y_{\pi 1}(x) - Y_{c1}(x)}{R_c(x) - R_\pi(x)} \tag{45}$$

$$G_{22}(x) = \frac{\frac{Y_{\pi 1}(x)}{R_c(x)} - \frac{Y_{c1}(x)}{R_\pi(x)}}{R_c(x) - R_\pi(x)}. \tag{46}$$

A design was analyzed that had the cross section shown in Fig. 15 and the following parameters:

$$l = 40 \text{ mm}$$
$$\epsilon_r = 3.82$$
$$R_1 = 325\ \Omega$$
$$R_2 = 175\ \Omega.$$

l, R_1, and R_2 were determined by iterating the analysis until the values of l, R_1, and R_2 used gave a 33 GHz center frequency and nearly equal power division across the band.

The software program by Djordjevic *et al.* [13] was used to iteratively determine values of $W_1(0)$, $S(0)$, and $W_2(0)$, and corresponding values $R_c(0)$, $R_\pi(0)$, $Y_{c1}(0)$, and $Y_{\pi 1}(0)$ that give $G_{11}(0)$, $G_{12}(0)$, and $G_{22}(0)$ corresponding to a π network composed of 50, 325, and 175 Ω resistances. The values obtained were

$$W_1(0) = 1.562 \text{ mm}$$
$$S(0) = 0.309 \text{ mm}$$
$$W_2(0) = 0.176 \text{ mm}$$
$$R_c(0) = 0.858$$
$$R_\pi(0) = -4.581$$
$$Y_{c1}(0) = 0.0204$$
$$Y_{\pi 1}(0) = 0.0372.$$

$W1(x)$, $S(x)$, and $W2(x)$ were chosen to vary according to

$$W_1(x) = W_1(0) + (W_1(l) - W_1(0))(x/l)^2 \tag{47}$$

$$S(x) = S(0) + (2W_1(l) - s(0))(x/l)^2 \tag{48}$$

$$W_2(x) = W_2(0) + (W_2(l) - W_2(0))(x/l)^2 \tag{49}$$

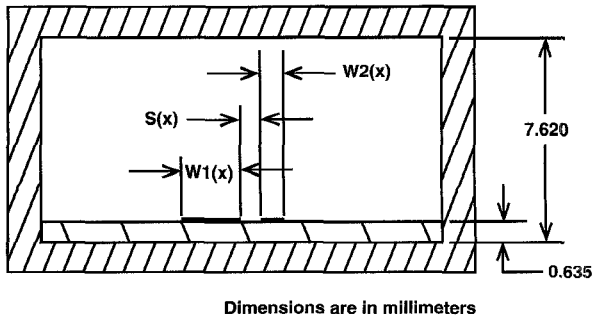

Fig. 15. Cross section of type 5 MLDD.

with $W_1(l) = W_2(l) = 1.392$ mm to give 50 Ω characteristic impedance at the outputs.

Theoretical performance was calculated for this design using the same type of analysis as for the type 3 and type 4

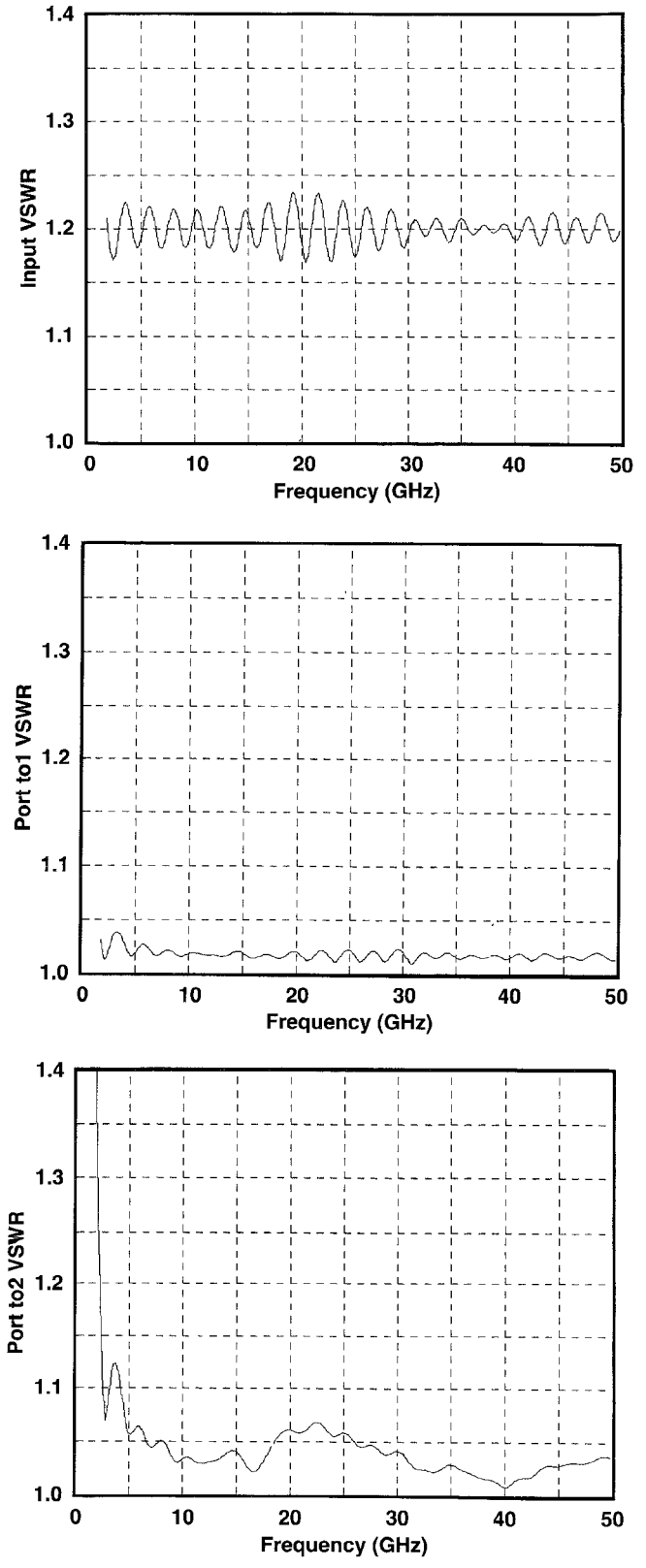

Fig. 16. Theoretical input (top) and output VSWR's (middle and bottom).

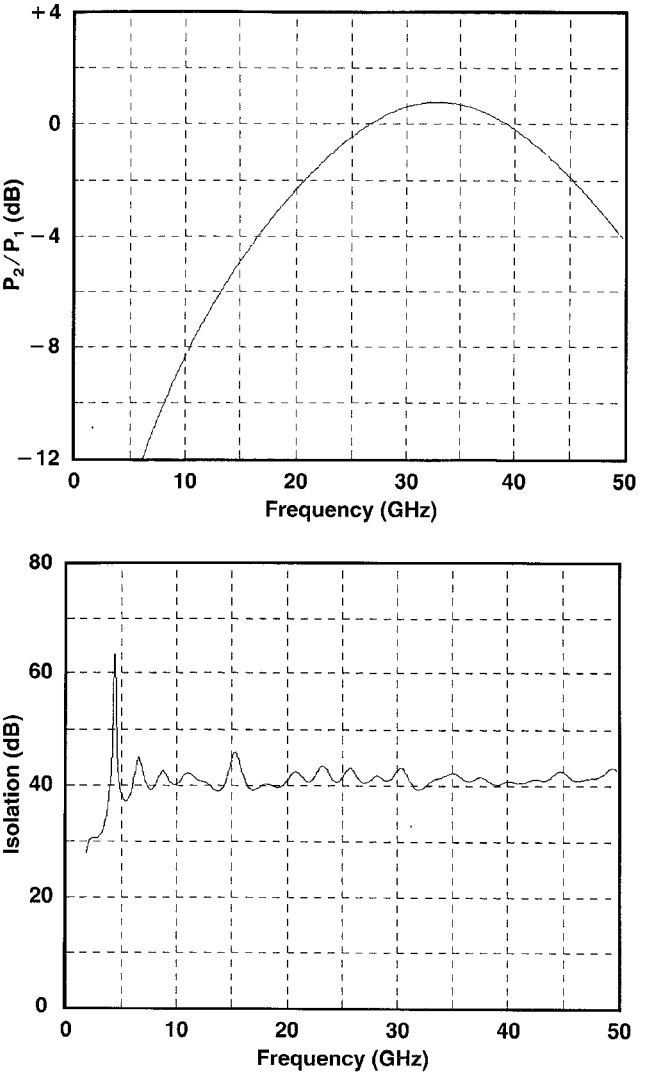

Fig. 17. Theoretical P_2/P_1 (top) and isolation (bottom).

MLDD's. Plots of input VSWR and output VSWR's are shown in Fig. 16. Plots of P_2/P_1 and isolation are shown in Fig. 17. P_2 and P_1 track within 0.8 dB from 24–42 GHz. Unlike conventional microstrip contradirectional couplers, isolation stays high over a broad frequency range and has a high-pass type of response. We will designate ϕ_1 to be the difference in phase between the signal at port $to2$ and the signal at port $to1$. ϕ_1 is plotted in Fig. 18. From 24–42 GHz ϕ_1 varies from $-35.2°$ to $+16.4°$. This variation suggests that this planar power divider would only be of interest when it was not required that the two outputs track in phase.

It is well known that a uniform section of transmission line introduces a negative phase shift that is proportional to frequency. By adding to port $to2$ a length of transmission line $l2 = 1.186$ mm, that introduces a phase shift of $-80.6°$ at 33 GHz, the output signals can be made to be 90° apart in phase. Let ϕ_2 designate ϕ_1 plus the phase shift introduced by line $l2$. ϕ_2 is plotted in Fig. 18. From 24–42 GHz ϕ_2 tracks $-90°$ within $\pm 4°$.

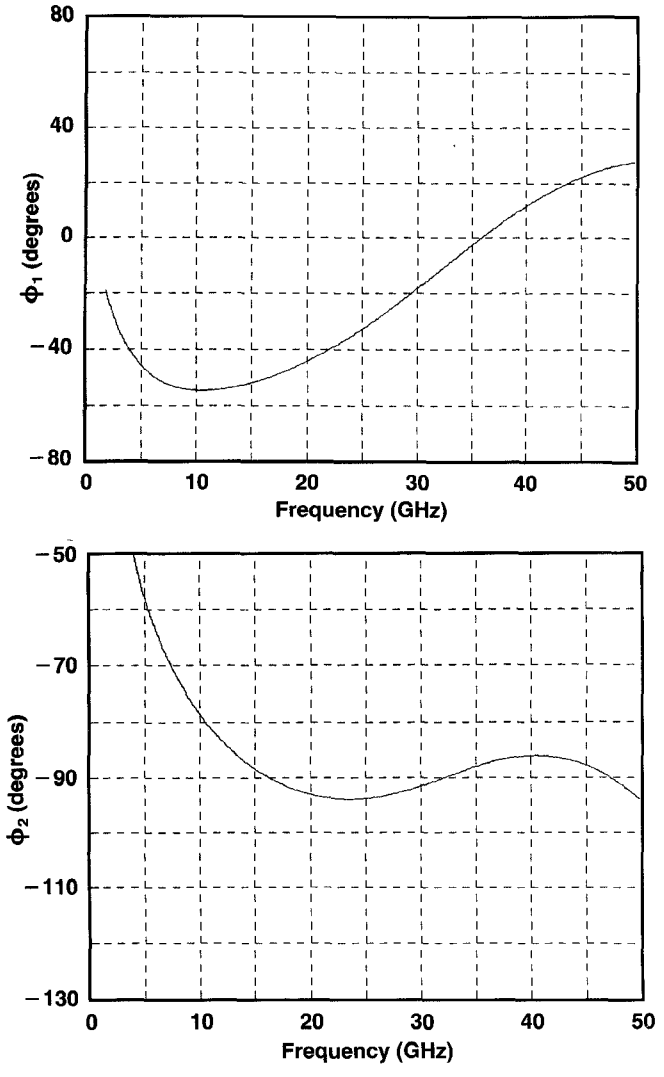

Fig. 18. Theoretical ϕ_1 (top) and ϕ_2 (bottom).

IX. Concluding Remarks

A new class of microwave devices—matched-line directional dividers—has been introduced that divides power from one input to two or more outputs, with the outputs isolated from each other.

Five types of MLDD's have been discussed. Inventive designers will undoubtedly generate many other types of MLDD's. The author is presently designing an MLDD that uses multiple dielectrics and gives 4-way equal power division over the 2–20 GHz frequency range.

The types 1, 2, 3, and 4 MLDD's demonstrate that, with homogeneous dielectrics, MLDD's can be designed to have high-pass responses and cover extremely broad frequency ranges. Measured results on the type 1 MLDD show it to outperform traditional Wilkinson–Cohn 2-way equal power dividers [1], [2] for very broadband high-frequency operation—giving lower insertion loss and higher isolation. However, for the majority of applications, which are below 20 GHz and 2 : 1 or under bandwidth, the well-designed Wilkinson–Cohn design gives excellent performance and is shorter in length and simpler to construct than the type 1 MLDD.

The types 3 and 4 MLDD's could also be referred to as codirectional directional couplers. For over 20 years, the author has specialized in the design for commercial sale of a wide variety of very broadband TEM-mode nonuniform tapered-line contradirectional stripline directional couplers [14]–[17]. The most difficult specification to meet on a continuing production basis has invariably been directivity. The main reason is that as frequency increases, the directivity of a very broadband TEM-mode stripline coupler increasingly degrades because of small differences in the even-mode and odd-mode phase velocities, since the directivity depends upon the cancellation of out-of-phase even-mode and odd-mode signals. These differences are caused by material variations and small air gaps that can occur between laminates. Directivity of the types 3 and 4 MLDD's are not significantly affected by these small material variations or air gaps since the directivity signal is eliminated by absorbtion in the input network resistors—not by cancellation of even-mode and odd-mode signals. Thus, very broadband stripline types 3 and 4 MLDD's can be expected to meet significantly higher directivity specifications on a production basis than TEM-mode stripline contradirectional couplers.

Another advantage of type 3 and 4 MLDD's is that ratio of the two outputs in the pass band is constant and does not have the ripple associated with conventional TEM-mode contradirectional couplers.

Theoretical analysis of a type 5 MLDD design predicts a microstrip 3 dB 90° hybrid covering the 24–42 GHz frequency range with high isolation and excellent amplitude and phase tracking.

For each of the MLDD designs discussed, output VSWR and isolation were optimized—at the price of a small nominal input VSWR. In each case, a lower nominal input VSWR could be traded for some degradation in output VSWR and isolation. It was felt that, in most practical designs, it would be more desirable to maximize output isolation, which also minimized output VSWR. This choice also simplified the theoretical analyses.

References

[1] E. J. Wilkinson, "An N-way hybrid power divider," *IRE Trans. Microwave Theory Tech.*, vol. MTT-8, pp. 116–118, Jan. 1960.
[2] S. B. Cohn, "A class of broadband three-port TEM-mode hybrids," *IEEE Trans. Microwave Theory Tech.*, vol. MTT-16, pp. 110–116, Feb. 1968.
[3] B. M. Oliver, "Directional electromagnetic couplers," *Proc. IRE* vol. 42, pp. 1686–1692, Nov. 1954.
[4] M. K. Krage and G. I. Haddad, "Characteristics of coupled microstrip lines—I: Coupled-mode formulation of inhomogeneous lines," *IEEE Trans. Microwave Theory Tech.*, vol. MTT-18, pp. 217–222, Apr. 1970.
[5] H. Amemiya, "Time-domain analysis of multiple parallel transmission lines,' *"RCA Rev.*, vol. 28, pp. 241–276, June 1967.
[6] R. E. Collin, "The optimum tapered transmission line matching section," *Proc. IRE,* vol. 44, pp. 539–548, Apr. 1956.
[7] R. W. Klopfenstein, "A transmission line taper of improved design," *Proc. IRE* vol. 44, pp. 31–35, Jan. 1956.
[8] S. B. Cohn and R. L. Levy, "History of passive components with particular attention to directional couplers," *IEEE Trans. Microwave Theory Tech.*, vol. MTT-32, pp. 1046–1054, Sept. 1984.
[9] V. K. Tripathi, "Asymmetric coupled transmission lines in an inhomogeneous medium," *IEEE Trans. Microwave Theory Tech.*, vol. MTT-23, pp. 734–739, Sept. 1975.
[10] R. A. Speciale and V. K. Tripathi, "Wave-modes and parameter matrices of non-symmetrical coupled lines in a non-homogeneous medium," *Int. J. Electronics,* vol. 40, no. 4, pp. 371–375, 1976.

[11] V. K. Tripathi and C. L. Chang, "Quasi-TEM parameters of nonsymmetrical coupled microstrip lines," *Int. J. Electronics,* vol. 45, no. 2, pp. 215–223, Aug. 1978.
[12] H. E. Green, "The numerical solution of some important transmission-line problems," *IEEE Trans. Microwave Theory Tech.,* vol. MTT-13, pp. 676–692, Sept. 1965.
[13] A. R. Djordjevic, T. K. Sarkar, R. F. Harrington, and M. B. Bazdar, *Matrix Parameters for Multi-Conductor Transmission Lines: Software and Users Manual.* Norwood, MA: Artech House, 1991.
[14] C. P. Tresselt, "The design and construction of broadband high-directivity 90-degree couplers using nonuniform line techniques," *IEEE Trans. Microwave Theory Tech.,* vol. MTT-14, pp. 647–656, Dec. 1968.
[15] G. L. Millican and R. C. Wales, "Practical strip-line microwave circuit design," *IEEE Trans. Microwave Theory Tech.,* vol. MTT-17, pp. 696–705, Sept. 1969.
[16] T. J. Russell, "High directivity TEM mode strip line coupler and method of making same," U.S. Patent 4,139,827, Feb. 13, 1979.
[17] ——, "Double-arrow 180° hybrid covers 2 to 18 GHz," *Microwave J.,* pp. 175–177, Mar. 1987.

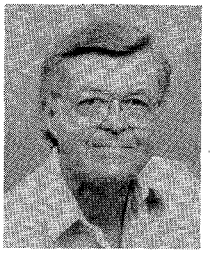

Thomas J. Russell (S'59–M'60) was born in Rock Rapids, IA, on June 13, 1933. He received the B.S. degree in electrical engineering from Iowa State University, Ames, in 1955, the M.S. degree in electrical engineering from the University of Missouri, Columbia, in 1960, and the M.S. degree in mathematics from the University of Missouri, Kansas City, in 1965.

From 1960 to 1966 he was with the Bendix Corporation, Kansas City, MO, working on the design of microwave components and test equipment. From 1966 to 1975 he was with Alfred Electronics Co., Palo Alto, CA, engaged in research and development of microwave components. He has been President of Krytar, Inc., Sunnyvale, CA, since co-founding the company in 1975. He has designed Krytar's complete line of broadband microwave components. He has published numerous papers and holds seven patents.

Mr. Russell is a member of Eta Kappa Nu.